第 50 卷 第 23 期/2023 年 12 月/中国激光 研究论文

中国激光

基于半导体碟片腔内倍频的高功率490 nm激光器

于圣杰[1]，冯健[1]，张新[1]，肖垚[2]，张志成[2]，王俊[2]，佟存柱[1*]

[1]中国科学院长春光学精密机械与物理研究所发光学及应用国家重点实验室，吉林 长春 130033；

[2]苏州长光华芯光电技术股份有限公司，江苏 苏州 215163

摘要 报道了基于半导体碟片激光倍频实现的高功率青色(蓝绿光)激光，连续输出功率可达到4.8 W。通过半导体碟片热管理优化和金刚石热沉预金属化，获得了最大功率为22.5 W、光-光转换效率为42.7%的980 nm基频光输出。通过V型腔LBO(LiB_3O_5)晶体倍频实现了4.8 W 490 nm激光输出，总的光-光转换效率为15.4%，单位泵浦面积产生的蓝绿光光强为3.8 kW/cm^2。

关键词 激光器；半导体碟片激光器；封装工艺；光泵浦；腔内倍频

中图分类号 TN248.4；TN365 **文献标志码** A **DOI**：10.3788/CJL230580

1 引 言

海水对470～580 nm波段的蓝绿光的衰减系数最小，而且490 nm附近是透射率峰值，因此蓝绿激光器在水下通信、水下激光探测以及水下激光雷达等方面[1]有着广阔的应用前景。蓝绿激光可以通过中红外激光四倍频、固体激光器和频、气体激光器和AlGaN半导体激光器直接激发及半导体碟片激光器倍频等方法实现[2-7]。半导体碟片激光器(SDLs)也称为垂直外腔面发射激光器(VECSELs)，它结合了半导体激光器和固体碟片激光器的优点，具有较小的体积和较高的输出功率。相较于固体激光材料而言，半导体材料具有对泵浦光的吸收效率更高、散热可控性更强、波长更丰富等优势。目前，通过扩大泵浦光斑尺寸以及对散热性能进行优化，1030 nm波长下最高可以实现百瓦功率输出[8]，通过腔内倍频在488 nm波长下可以实现15 W功率输出[9]。

半导体激光器受温度影响严重，良好的热管理是提高激光器性能的关键。半导体碟片激光器通常通过表面散热和倒装焊接的方式提高散热能力，但是表面散热对表面散热片的要求较高，而且散热片价格昂贵；倒装焊接使用镀制Ti-Pt-Au的金刚石作为热沉来提高散热能力，但是在蒸镀过程中铂易在金刚石表面凝结，影响封装质量，导致热阻增加，使激光器的散热能力减弱，阻碍功率的提高。

笔者报道了一种半导体碟片激光器，通过对金刚石进行预金属化处理，改善了封装质量，实现了高功率激光输出；通过搭建V型腔并在腔内插入LiB_3O_5(LBO)晶体用于腔内倍频，实现了高功率490 nm蓝绿激光输出。

2 半导体碟片激光器设计封装

2.1 半导体碟片结构的设计及仿真

所研究的半导体碟片激光器是基于GaAs基片外延生长的，如图1所示，其结构主要包括三部分：1) 用于限制载流子外泄和起保护作用的盖层；2) 用于提供增益的有源区量子阱；3) 用于对目标波长实现谐振反馈的分布式布拉格反射镜(DBR)。其中量子阱有源区结构采用了双量子阱结构，以最大限度地提高增益，使用6对InGaAs双量子阱层，共12个量子阱。

在有源区的设计中，通过势垒层厚度的调控调节量子阱之间的光学距离，以确保在空间位置上量子阱

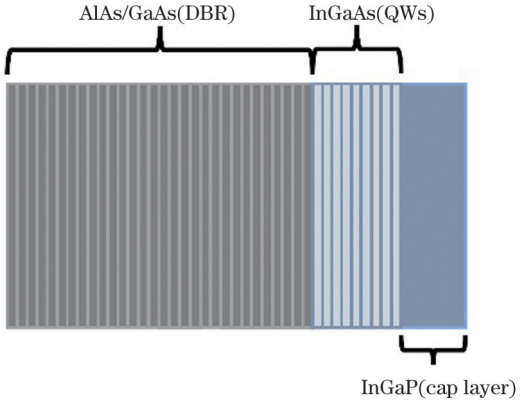

图1 半导体碟片激光器的外延结构

Fig. 1 Epitaxial structure of semiconductor disk laser

收稿日期：2023-03-02；**修回日期**：2023-04-07；**录用日期**：2023-04-11；**网络首发日期**：2023-04-25

基金项目：国家自然科学基金杰出青年基金(62025506)

通信作者：*tongcz@ciomp.ac.cn

与微腔内的驻波场波腹位置重叠进而实现周期性共振增强结构(RPG),DBR 高反射膜层则采用 26 对未掺杂的 AlAs/GaAs 层,以确保对目标波长实现高的反射率,如图 2 所示。

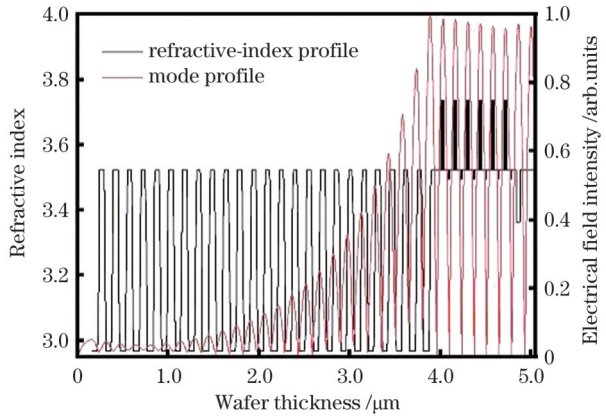

图 2 器件外延结构的折射率及光场分布

Fig. 2 Refractive index and optical field distribution of epitaxial structure of the device

2.2 半导体碟片激光器的热管理及封装工艺

光泵浦半导体碟片连续激光器采用的是势垒泵浦的方法,较大的势垒厚度有助于对泵浦光的吸收。通过测量可知有 70% 的泵浦光被吸收,30% 的泵浦光被反射。采用势垒泵浦虽然增强了吸收,但势垒与量子阱基态能级之间存在较大能级差的无辐射跃迁,这会导致自热产生,进而导致温度升高,并进一步导致俄歇复合和载流子逃逸,使器件量子效率降低,进一步导致器件发生热反转功率下降。因此,热问题是一直都是限制半导体激光器功率增大的关键。为此,需要优化碟片激光器的热沉等封装结构。

本次实验采取倒置的方式,以避免低热导率衬底的影响。倒置方案如图 3 所示,热量由有源区通过 DBR 层、键合层和热沉传导至散热器表面。为实现高效散热,需要调节有源区到散热器表面的厚度、热阻以及键合质量。实验中采用具有高热导率的金刚石作为导热材料,使用 Ti-Pt-Au 作为键合层,利用金与铟的固液相互扩散键合实现芯片与金刚石的键合,其中铂具有扩散媒介的作用,以便形成合金,达到键合的目的。该方法已经实现了高功率输出[8],但是在实验中笔者发现该方法仍存在一定问题:铂在电子束蒸发期间倾向于扩散到金刚石表面并凝结形成点,导致封装质量下降,热阻增大。为改善封装质量,选用高热导率的 CuSn 合金作为阻挡层[10],增加铂与金刚石之间的厚度,阻止铂在金刚石表面凝结。结合碟片热管理及工艺需要,笔者对半导体碟片封装工艺进行了改进。

在对金刚石热沉进行清洁之后,将其放入 VNANO 公司生产的型号为 VZZ-300S 的高真空电阻式蒸发镀膜机中,将金刚石加热至 200 ℃后蒸镀 50 nm 的 $Cu_{85}Sn_{15}$ 合金薄膜,沉积速率为 0.5 nm/s。在对金刚石上下表面预金属化后,继续生长 60 nm/60 nm/250 nm 的 Ti-Pt-Au。对金刚石完成金属化后,对芯片及铜热沉蒸镀 5 μm 厚的铟层,然后使用共晶回流焊设备将芯片、金刚石以及铜热沉封装在一起。图 3 所示为半导体碟片封装结构,其中图 3(a)为金刚石热沉金属化及键合结构,图 3(b)为封装后的半导体碟片激光器。

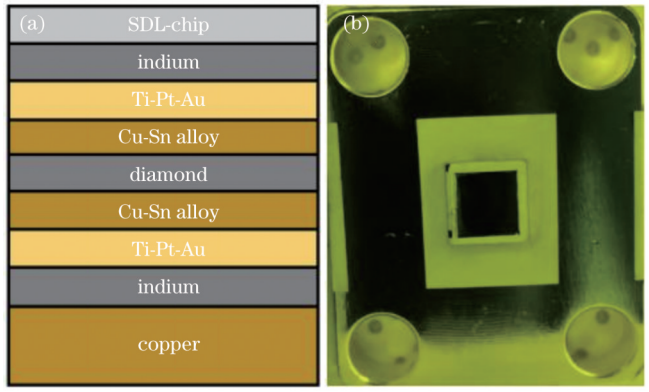

图 3 半导体碟片封装结构。(a)金刚石金属化及键合结构;(b)封装后的半导体碟片激光器

Fig. 3 Semiconductor disk package structure. (a) Metallization and bonding structure of diamond; (b) packaged semiconductor disk laser

3 实验结果与分析

采用 I 型直腔测试半导体碟片激光器的性能,同时采用 V 型腔实现半导体碟片激光器的倍频输出,如图 4 所示。

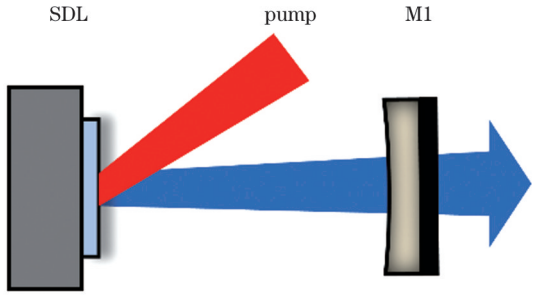

图 4 直腔结构半导体碟片激光器

Fig. 4 Direct-cavity semiconductor disk laser

输出耦合镜 M1 是曲率半径为 100 mm 的平凹镜,其对基频光的透过率为 3%,I 型直腔的腔长为 90 mm。使用波长为 808 nm、最高功率为 240 W、芯径为 200 μm 的光纤激光器进行表面泵浦,聚焦在碟片表面的泵浦光斑的直径为 400 μm。碟片通过半导体制冷片进行散热,温度设置为 10 ℃。

分别对激光器的功率输出特性和光谱特性进行测试。对半导体碟片进行表面泵浦时存在 30% 的反射,因此后面在介绍泵浦功率时,均为减去 30% 表面反射后的吸收泵浦功率。从图 5 所示输出功率曲线可以看到:激光器的斜率效率为 47.3%;在吸收泵浦功率达到

52.7 W时，输出功率达到了22.5 W，总的光-光转换效率为42.7%。

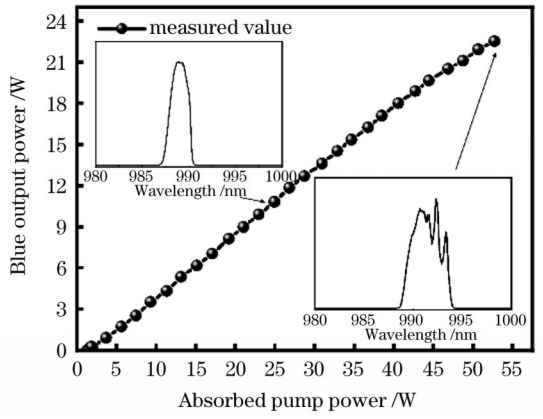

图5 光泵浦半导体碟片激光器的功率和光谱特性

Fig. 5 Power and spectral characteristics of an optically pumped semiconductor disk laser

倍频效率主要受基频光功率、晶体位置处的束腰尺寸、非线性晶体本身特性等因素的影响。得益于半导体碟片激光器的外腔结构，可以通过腔体设计及腔内倍频的方式，在晶体位置处获得小尺寸束腰，提高倍频晶体处基频光的功率密度。图6和图7所示为倍频时采用的V型腔结构示意图以及腔内光斑尺寸与腔内位置的关系。

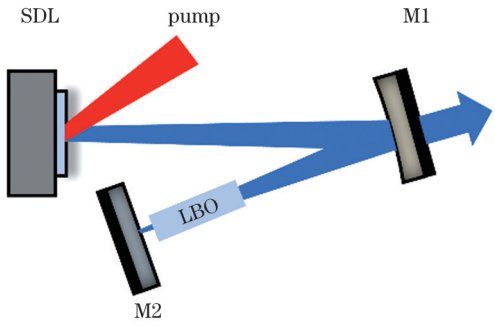

图6 V型腔结构示意图

Fig. 6 Schematic diagram of V-shaped cavity structure

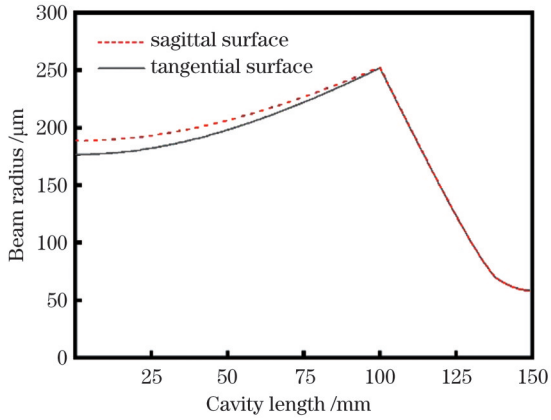

图7 光斑尺寸与腔内位置的关系

Fig. 7 Relationship between spot size and cavity position

M1镜是曲率半径为77.5 mm的平凹镜，其表面镀制996 nm 99.5%的增反膜和498 nm 99.5%的增透膜后作为倍频光输出镜；M2镜是平行平面镜，其表面镀制996 nm和498 nm 99.5%的双增反膜。实验中采用的V型腔腔体展开后总腔长为150 mm。图7中，虚线为弧矢面，实线为切线面。从图7中可以看出在腔内位置为150 mm处的光斑半径为58.5 μm，即M2平行平面镜处。非线性晶体特性如走离角、接收带宽范围和温度接收范围等参数对倍频效率的影响较大，为获得较高的倍频效率，采用走离角小以及温度接收范围和接收带宽大的LBO晶体[11]，LBO晶体的尺寸为3 mm×3 mm×10 mm。将非线性LBO晶体放置于M2镜前1 mm处，晶体中心位置处的光斑半径为62 μm。因为是连续激光器，存在热累积，为避免晶体温度过高导致晶体热透镜效应和相位匹配失配等问题，使用半导体制冷片(TEC)对晶体进行温度控制，温度设置为10 ℃。使用二向分色镜进行滤光，使用功率计和光谱分析仪对倍频输出功率和光谱特性进行分析。如图8所示，蓝绿光输出的斜率效率为17.8%，最大输出功率达到4.8 W，总的光-光转换效率为15.4%。如图9所示，倍

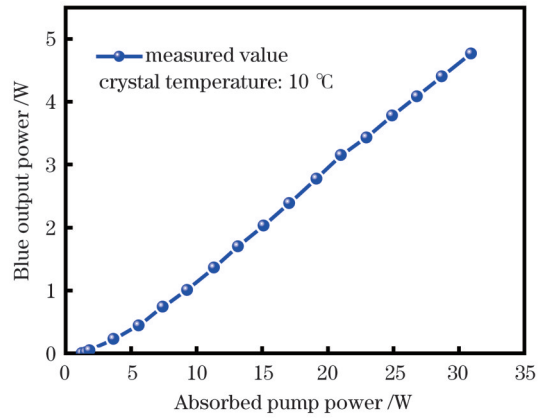

图8 蓝绿光倍频功率特性曲线

Fig. 8 Frequency doubling power characteristic curve of blue green light

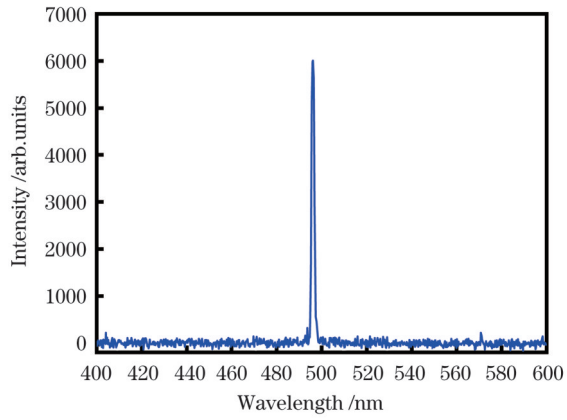

图9 蓝绿光的光谱特性

Fig. 9 Spectral characteristic of blue and green light

频后蓝绿光波长为496.1 nm。碟片表面的泵浦光斑直径为400 μm，在该泵浦光尺寸下，最大蓝绿光输出功率下单位泵浦面积产生的倍频光光强为3.8 kW/cm^2。

表1汇总了490 nm光泵浦半导体碟片激光器国内外实验研究结果，可以看出倍频光的功率与泵浦光斑面积密切相关。Chilla等[9]通过大的泵浦光斑直径（约800 μm）获得了30 W基频光和15 W倍频光，单位泵浦面积产生的倍频激光光强为2.98 kW/cm^2，而通过直径为120 μm的泵浦光斑只能实现百毫瓦量级的激光输出。本工作中泵浦光斑的直径为400 μm，获得了22.5 W基频光和4.8 W的倍频光，对应最大单位泵浦面积的倍频激光光强为3.8 kW/cm^2。相较于Chilla等[9]的结果，笔者设计的碟片激光器具有更高的单位面积倍频光强，说明其单位面积的热导更好。但该碟片激光器的倍频光功率和效率还存在差距，后续拟将进一步增大泵浦光斑面积。

表1 490 nm光泵浦半导体碟片激光器腔内倍频实验结果对比

Table 1 Comparison of 490 nm lasers by intracavity frequency doubling of semiconductor disk lasers

Wavelength / nm	Pump power /W	Pump-spot size /μm	Maximum power of basic-frequency light /W	Maximum power of second harmonic generation (SHG) /W	Conversion efficiency /%
488[12]	3.68	120	1.12	0.11	1.7
488[9]	54.5	800	30	15	27.5
492	30.9	400	22.5	4.8	15.4

4 结 论

报道了一种可以极大改善半导体碟片激光器散热能力的封装工艺，该工艺可以抑制封装过程中铂在金刚石表面凝结的问题，使激光芯片与金刚石热沉结合得更加紧密，降低了器件的热阻，提高了散热能力。通过该封装工艺，在400 μm泵浦光斑直径下，获得了功率为22.5 W的基频光输出，最大输出功率下的光光转换效率为42.7%；通过V型腔进行倍频获得了4.8 W的蓝绿光输出，总的光光转换效率为15.4%，单位泵浦面积产生的蓝绿光光强为3.8 kW/cm^2。

参 考 文 献

[1] 曾凤娇, 杨康建, 晏旭, 等. 水下激光通信系统研究进展[J]. 激光与光电子学进展, 2021, 58(3): 0300002.
Zeng F J, Yang K J, Yan X, et al. Research progress on underwater laser communication systems[J]. Laser & Optoelectronics Progress, 2021, 58(3): 0300002.

[2] Xu L, Liang S J, Fu Q, et al. Highly efficient frequency doubling and quadrupling of a short-pulsed thulium fiber laser[J]. Applied Physics B, 2018, 124(4): 59.

[3] 王君光, 李永亮, 田迎华, 等. 全固态腔内和频488 nm连续蓝光激光器[J]. 中国激光, 2010, 37(7): 1669-1672.
Wang J G, Li Y L, Tian Y H, et al. All-solid-state continuous-wave all-intracavity sum-frequency mixing blue laser at 488 nm[J]. Chinese Journal of Lasers, 2010, 37(7): 1669-1672.

[4] Gerritsen H J, Goedertier P V. Blue gas laser using Hg^{2+} [J]. Journal of Applied Physics, 1964, 35(10): 3060-3061.

[5] 胡磊, 张立群, 刘建平, 等. 高功率氮化镓基蓝光激光器[J]. 中国激光, 2020, 47(7): 0701025.
Hu L, Zhang L Q, Liu J P, et al. High power GaN-based blue lasers[J]. Chinese Journal of Lasers, 2020, 47(7): 0701025.

[6] Ostroumov V, Simon C, Schwarze H, et al. 1 W 488 nm cw air-cooled optically pumped semiconductor laser[J]. Proceedings of SPIE, 2008, 6871: 687118.

[7] 马剑, 朱小磊, 陆婷婷, 等. 海洋应用高峰值功率蓝光脉冲激光器技术研究[J]. 光学学报, 2022, 42(17): 1714002.
Ma J, Zhu X L, Lu T T, et al. Research on pulsed blue laser with high peak power for ocean applications[J]. Acta Optica Sinica, 2022, 42(17): 1714002.

[8] Heinen B, Wang T L, Sparenberg M, et al. 106 W continuous-wave output power from vertical-external-cavity surface-emitting laser[J]. Electronics Letters, 2012, 48(9): 516-517.

[9] Chilla J L A, Butterworth S D, Zeitschel A, et al. High-power optically pumped semiconductor lasers[J]. Proceedings of SPIE, 2004, 5332: 143-150.

[10] Hou G Y, Shu S L, Feng J, et al. High power (>27 W) semiconductor disk laser based on pre-metalized diamond heat-spreader[J]. IEEE Photonics Journal, 2019, 11(2): 1501908.

[11] Lin Z S, Lin J Y Y, Wang Z Z, et al. Mechanism for linear and nonlinear optical effects in LiB_3O_5, CsB_3O_5, and $CsLiB_6O_{10}$ crystals[J]. Physical Review B, 2000, 62(3): 1757-1764.

[12] 王菲. 高稳定度光泵浦腔内倍频488 nm半导体薄片激光器[J]. 红外与激光工程, 2019, 48(6): 0606004.
Wang F. High stability 488 nm light generated by intra-cavity frequency doubling in optically pumped semiconductor disc lasers [J]. Infrared and Laser Engineering, 2019, 48(6): 0606004.

High Power 490 nm Laser Based on Semiconductor Disk Intracavity Frequency Doubling

Yu Shengjie[1], Feng Jian[1], Zhang Xin[1], Xiao Yao[2], Zhang Zhicheng[2], Wang Jun[2], Tong Cunzhu[1*]

[1]*State Key Laboratory of Luminescence and Applications, Changchun Institute of Optics, Fine Mechanics and Physics, Chinese Academy of Sciences, Changchun* 130033, *Jilin, China*;

[2]*Suzhou Everbright Photonics Co., Ltd., Suzhou* 215163, *Jiangsu, China*

Abstract

Objective The attenuation coefficients of blue and green light in the 470–580 nm band are the smallest in seawater, especially at the peak of transmittance near 490 nm. Therefore, blue-green lasers have important application prospects in underwater communications, laser detection, and radars. Currently, blue-green lasers can be realized using a middle-infrared laser quadruple frequency, solid-state laser sum frequency, and gas laser and AlGaN semiconductor laser direct excitation. However, these methods have low energy conversion efficiency and poor beam quality. The advantages of semiconductor disk lasers used to produce blue and green lasers are good beam quality, high-frequency doubling efficiency, and improved stability and reliability. The thermal problem is a key factor affecting the performance of semiconductor disk lasers and must be improved by optimizing the packaging structure. The semiconductor disk packaging process uses Ti-Pt-Au as the bonding layer and realizes bonding between the chip and diamond by the solid-liquid diffusion bonding of gold and indium. Pt acts as a diffusion medium for bonding. The experiment conducted herein identified that this method has some problems. Pt tends to spread onto the diamond surface and condense to form points during electron-beam evaporation. Packaging quality decreases and thermal resistance increases, limiting laser performance improvement.

Methods The epitaxial structure of the 980 nm semiconductor disk consists of 26 pairs of distributed Bragg reflectors with undoped AlAs/GaAs layers, six pairs of active regions with InGaAs double quantum wells, and a high bandgap energy cap layer (Fig. 1). The quantum well spatial position in the epitaxial structure of the semiconductor disk must coincide with the standing-wave peak at the designed wavelength (Fig. 2). Based on the Ti-Pt-Au packaging technology, a Cu-Sn alloy with high thermal conductivity is selected as the barrier layer to increase the thickness between Pt and diamond. Pt is prevented from condensing on the diamond surface and the packaging process is improved. A 490 nm laser with high power is obtained by constructing a V-shaped cavity and using an LBO crystal cavity with intracavity frequency doubling (Fig. 6).

Results and discussions A direct cavity is used to test the performance of the semiconductor disk laser. The output coupler M1 is a concave mirror with curvature radius of 77.5 mm and reflectance coating of 97%. The resonator cavity length is 90 mm (Fig. 4). A fiber laser of 808 nm wavelength of is used as the pump source and the spot size is 400 μm. The temperature of the chip is controlled using a thermoelectric cooler (TEC) and the temperature is set to 10 ℃. The laser slope efficiency reaches 47.3%. When the absorption pump power reaches 52.7 W, the output power will reach 22.5 W. The total optical-to-optical conversion efficiency is 42.7% (Fig. 5). The V-shaped cavity is used for second harmonic generation output. The output coupler M1 is a concave mirror with curvature radius of 77.5 mm, the reflection film of 996 nm 99.5% and antireflection film of 498 nm 99.5% are coated. M2 is a parallel-plane mirror-plated 996 and 498 nm 99.5% reflection film. The size of the LBO crystal is 3 mm×3 mm×10 mm (Fig. 6). The temperature of the crystal is controlled using a thermoelectric cooler (TEC) and the temperature is set to 10 ℃. The slope efficiency of the blue and green light output is 17.8%, the maximum output power is 4.8 W and the total optical-optical conversion efficiency is 15.4% (Fig. 8). After frequency doubling, the wavelength of the blue and green light is 496.1 nm (Fig. 9). The pump spot on the surface of the disk has a 400 μm diameter. Under the spot size, the maximum output power of blue and green light produces a frequency-doubling light intensity of 3.8 kW/cm^2 per unit pumping area. This study compares the experimental results of a 490 nm optically pumped semiconductor disk laser at home and abroad (Table 1). In this research, a high fundamental frequency optical power and higher frequency doubling light intensity per unit area are obtained under a higher pump power density, indicating that the proposed chip unit area has an improved heat dissipation capacity. The frequency-doubling light power and efficiency reported in this study can be improved and the pump spot area can be further increased in the future.

Conclusions A packaging process is developed that significantly improves the heat dissipation capacity of semiconductor disk lasers. This packaging technology can suppress Pt condensation on diamond surfaces during packaging. This packaging process bonds the laser chip and diamond heat sink more closely, reduces device thermal resistance, and improves heat-dissipation capacity. A fundamental-frequency optical output of 22.5 W with a pump spot diameter of 400 μm is obtained using the packaging process. The optical conversion efficiency is 42.7% at the maximum output power. A blue and green light output of 4.8 W is obtained through frequency doubling. The total optical-optical conversion efficiency is 15.4%, and the intensity of blue and green light produced per unit pumping area is 3.8 kW/cm^2.

Key words lasers; semiconductor disk laser; packaging process; optical pumping; intracavity frequency doubling